COMBINATORIAL INVESTIGATION OF STRUCTURAL AND FERROELECTRIC PROPERTIES OF A- AND B-SITE CO-DOPED BiFeO$_3$ THIN FILMS

DAISUKE KAN [a]; RICHARD SUCHOSKI [a]; SHIGEHIRO FUJINO [a]; ICHIRO TAKEUCHI [a]

[a] Department of Materials Science and Engineering, University of Maryland, College Park, MD, U.S.A.

Online publication date: 18 March 2010

PLEASE SCROLL DOWN FOR ARTICLE

Combinatorial Investigation of Structural and Ferroelectric Properties of A- and B-Site Co-Doped BiFeO₃ Thin Films

Daisuke Kan, Richard Suchoski, Shigehiro Fujino, and Ichiro Takeuchi*

Department of Materials Science and Engineering, University of Maryland,
College Park, MD 20742, U.S.A.

We have systematically investigated structural and ferroelectric properties of A- and B-site co-doped BiFeO₃ thin films using the composition spread technique. X-ray diffraction and polarization hysteresis loop measurements reveal that the co-doped $(Bi,Sm)(Fe,Sc)O_3$ exhibits the structural transition from the rhombohedral to an orthorhombic structural phase which is accompanied by a double-hysteresis behavior in the polarization hysteresis loop. We find that the phase transition takes place at Sm ∼14% independent of the Sc composition. This clearly indicates the significance of the A-site dopant on structural and ferroelectric properties in BiFeO₃.

INTRODUCTION

Perovskite bismuth ferrite BiFeO₃ (BFO) [1, 2] which exhibits simultaneous coexistence of ferroelectricity ($T_c \sim 1103$ K) and antiferromagnetism ($T_N \sim 643$K) at room temperature has drawn considerable attention. Substitution of rare earth (RE), for example La, Gd, and Dy [3–8] into BFO has frequently been attempted aiming at improving ferroelectric properties such as high leakage current and large coercive fields which are known to be shortcomings of BFO.

Recently, we have discovered [9] a universal behavior in structural and ferroelectric properties in RE (= Sm, Gd, Dy) substituted BFO, where changes in structural and ferroelectric properties can be described using one parameter, the average A-site ionic radius. With increasing the RE composition, the rhombohedral structure of BFO undergoes a structural transition to an orthorhombic structure with a dimension of $\sqrt{2}a_0 \times \sqrt{2}a_0 \times 2a_0$ where a_0 is the pseudo-cubic lattice parameter. At the phase boundary, the ferroelectric properties in the

---

*Corresponding author. E-mail: takeuchi@umd.edu

rhombohedral phase are consequently changed to paraeelctric properties in an orthorhombic phase, exhibiting double hysteresis behavior in the polarization-electric field (PE) hysteresis loop, and there is concomitant enhancement of both piezoelectric coefficient d_{33} and dielectric constant ε_{33}. The maximum d_{33} is as high as 110 pm/V [10] which is comparable to that of single-domain $Pb(Zr_{0.5}Ti_{0.5})O_3$ thin films [11]. These results indicate that in the RE-substituted BFO, the chemical pressure effect due to the substitution, which induces tilting of oxygen octahedra and stabilizes the orthorhombic structure [12], is crucial for its structural transition and the concomitant changes in ferroelectric properties. According to the tolerance factor framework, it is possible to induce similar tilting of oxygen octahedra by the B-site substitution. However, to date the B-site substitution effect in BFO has not been fully investigated.

Since the ferroelectric polarization mainly results from the 6s lone pair [13] of the Bi ion in the A-site, introduction of dopants into B-site is expected to improve ferroelectric and dielectric properties without losing fundamental structural and ferroelectric properties of $BiFeO_3$. In this study, we have investigated the B-site substitution effect on the structural and ferroelectric properties in $(Bi,Sm)FeO_3$ by means of the thin-film composition spread technique. We have chosen Sc as the substitutional dopant for the B-site [14]. A Sc ion has a robust 3+ valence state which is unlikely to cause an increase in leakage current. The ionic radius of Sc^{3+} in 6 coordination is 0.745 Å which is larger than the one for Fe^{3+}, 0.645 Å. The tolerance factor framework predicts that substitution of a lager dopant into the B-site would be likely to induce distortions or tilting of the oxygen octahedral in the perovskite lattice. Indeed, the end material $BiScO_3$ has a distorted orthorhombic structure with a dimension of $2\sqrt{2}a_0 \times \sqrt{2}a_0 \times 4a_0$ [15]. Scanning xray diffractions (XRD) and PE hysteresis loop measurements show that the fabricated ternary library of A-site and B-site co-doped BFO exhibits the structural transition from the rhombohedral to the orthorhombic phase, accompanied with double-hysteresis behavior in PE hysteresis loops. Based on experimental results, the effect of B-site substitution on the structural transition in BFO is discussed.

EXPERIMENTAL

We employed a combinatorial approach to systematically investigate structural and ferroelectric properties of the A- and B-site co-doped $(Bi,Sm)(Fe,Sc)O_3$. The 200-nm thick ternary composition spread library was fabricated on a (001) $SrTiO_3$ substrate buffered with a 50 nm thick $SrRuO_3$ which serves as the bottom electrode. The library was fabricated using a combinatorial pulsed laser deposition system with an automated shadow mask and a multi targets system. Figure 1 shows a design schematic of the fabricated library. In this design, concentration of the each dopant (A- or B-site dopant) varies along one of the sides of the triangle. This allows us to separate the A-site and B-site
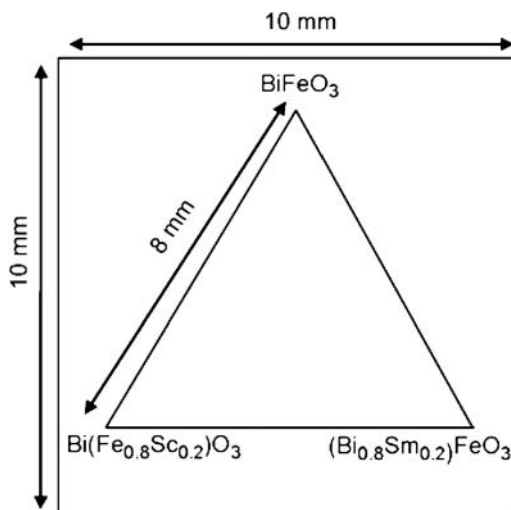
Figure 1. Design schematic of the fabricated library. The equilateral triangle-shaped library with a side length of 8 mm was made on a substrate that is 10 mm by 10 mm in size. The compositions shown here were determined by the electron probe.

substitution effect. During the deposition of the library, the substrate temperature and oxygen pressure were kept at 600 °C and 25 mTorr, respectively. Ceramic sintered pellets of $Bi_{1.1}FeO_3$, $SmFeO_3$ and $BiScO_3$ were used as starting materials. Structural characterization was performed with scanning x-ray micro-diffraction with a 2-dimensional detector (Bruker D8). The x-ray beam spot was focused into 0.5 mm φ with an aperture. The compositions across the library were determined by an electron probe (JEOL JXA-8900) with the uncertainty of $+/-$ 1.5% in composition at each point. For electrical characterization, a 100-nm thick Pd top electrodes layer was sputtered and patterned through a conventional lift-off process at room temperature. PE hysteresis loops were acquired at 5 kHz with Radient Premiere II at room temperature. Top electrodes with the size of $50 \times 50 \ \mu m^2$ are 250 μm apart horizontally and 200 μm apart vertically on the library as shown in Fig. 1.

RESULTS AND DISCUSSIONS

The scanning 2-dimensional XRD reveals structural evolution due to the substitutions. Figures 2(a)-(c) show representative 2-dimensional XRD images taken for the library with the incident x-ray parallel to the $[100]_{STO}$ direction. The vertical and horizontal axis in the image is parallel to the $[001]_{STO}$ and the $[010]_{STO}$ direction, respectively. For pure BFO (Fig. 2(a)), (00L) fundamental Bragg reflections from the film and the substrate are observed, which confirm
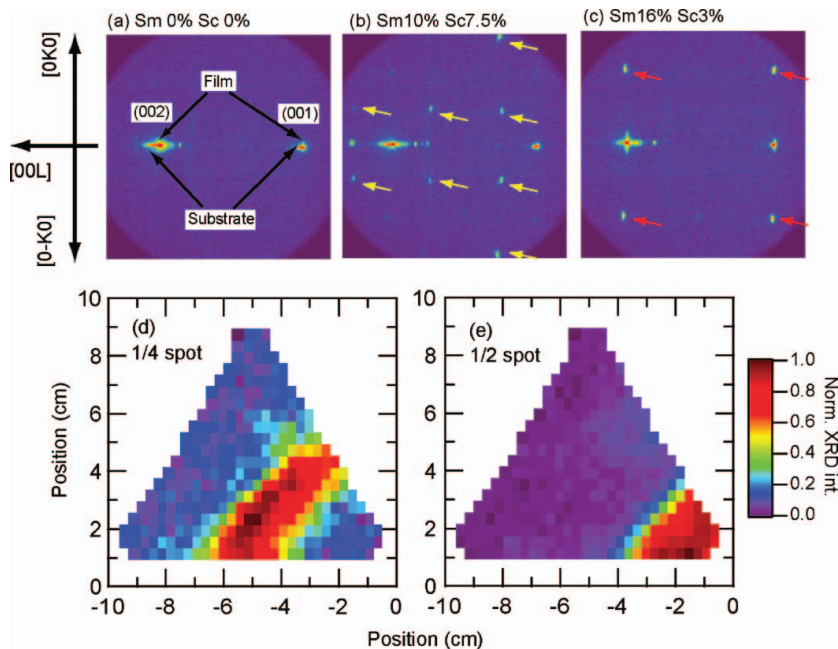
Figure 2. Representative 2-dimensional x-ray diffraction patterns taken for the fabricated library (a)-(c). The substituting compositions are (a) Sm 0%, Sc 0%, (b) Sm 10%, Sc 7.5%, and (c) Sm 16%, Sc 3%. The diffraction spots indicated by yellow and red arrows are assigned as $\frac{1}{4}\{011\}$ and $\frac{1}{2}\{010\}$ spots, respectively. In (d) and (e), the normalized intensities of (0, 1/4 7/4) ($\frac{1}{4}\{011\}$) and (0, 1/2, 2) ($\frac{1}{2}\{010\}$) are displayed. The intensities are plotted against the position in the library. (See Color Plate XXXII)

epitaxial growth of the film on the substrate. As the doping concentrations are increased, two types of key diffraction spots emerge as seen in Figs. 2(b) and 2(c). One type is 1/4{011} spots seen in Fig. 2(b) (marked with yellow arrows), and the other is 1/2{010} spots seen in Fig. 2(c) (marked with red arrows). From extensive XRD and TEM studies using binary composition spreads and single composition films of RE-doped BFO thin films [9,12], it was revealed that the 1/4{011} spots arise from the anti-parallel cation displacements which occur in local regions typically 10–20 nm in size (and not entire bulk matrix of the film). The 1/2{010} spots result from an orthorhombic structural phase with a dimension of $\sqrt{2}a_0 \times \sqrt{2}a_0 \times 2a_0$, where the film grows with $(110)_{ortho}$ orientation and the $[001]_{ortho}$ axis is parallel to either the $[100]_{STO}$ or $[010]_{STO}$ axis.

Figures 2(d) and (e) show normalized intensity plots of the 1/4{011} and 1/2{010} spots, respectively. The region where these extra spots are observed lies at the right bottom in the library. This indicates that without the Sm dopants into A-site in the BFO lattice, the rhombohedral to orthorhombic

structural transition dose not take place in the composition range studied here. The impact of Sm doping on the structural transition is confirmed by the fact that the occurrence of the 1/4 and 1/2 spots takes place as one goes down the side of the library where Sm concentration is varied continuously.

As the substitution concentration is continuously increased starting from the undoped composition, first the 1/4 spot begins to appear. With further substitution, the 1/4 spot eventually gets diminished and disappear altogether, while the 1/2 spot gets enhanced. The composition region between where the 1/4 and 1/2 spot intensities are seen corresponds to the structural transition boundary from the rhombohedral to the orthorhombic phase. This behavior is consistent with the structural evolution observed in RE-substituted BFO where RE = Sm, Gd and Dy [9].

Ferroelectric properties also exhibit concomitant changes in response to the structural evolution. In Fig. 3(a), we present all room-temperature PE hysteresis loops taken across the library displayed at the positions of the top electrodes. For each loop, the horizontal axis spans -500 to 500 kV/cm for electric field, and the vertical axis is from -120 to 120 μC/cm^2 for polarization. In the region with lower dopant compositions, the unclosed loops are observed indicating that leakage current is too high. As the substitution of Sm and Sc is increased, the square-shaped ferroelectric hysteresis loop with the saturation polarization of about 70 μC/cm^2 begins to appear. This indicates that the substitution helps to reduce the leakage current. The fact that in the composition region where only Sc is substituted, the hysteresis loops observed are ones characteristic of leaky ferroelectrics suggests that the Sm doping is effective in reducing the leakage current as compared to the Sc doping.

As the Sm substitution reaches 14%, the ferroelectric hysteresis loops undergo a transition to double-hysteresis loops. The transition from the single to the double-hysteresis loop is clearly seen in the Fig. 3(b) where the PE hysteresis loops in the red box in Fig. 3(a) are separately plotted. The ferroelectric hysteresis loop becomes distorted and the double-hysteresis behavior begins to appear as the Sm composition approaches 14%. Beyond this composition, the fully-developed double-hysteresis loops are observed. The observed behavior is in good agreement with previous observations for Sm-doped BiFeO$_3$ thin films [9, 10, 12]. Based on the first principles calculations [9], it was proposed that the double hysteresis loop arises from an electric-induced structural transition from the non-polar orthorhombic to the polar rhombohedral phase. Our observations imply that the B-site substitution doesn't affect this mechanism as long as the rhombohedral to orthorhombic structural transition happens. As in the case of the structural transition, the evolution in the ferroelectric properties also takes place along the Sm composition axis and confirms that the substitution on A-site plays the main role on the both structural and ferroelectric properties.

To fully illustrate the substitution effect of A-site and B-site on the structural and the ferroelectric properties in $(Bi,Sm)(Fe,Sc)O_3$, we plotted normalized intensities of (0, 1/4, 7/4) (referred to as 1/4) and (0, 1/2, 2) (referred to
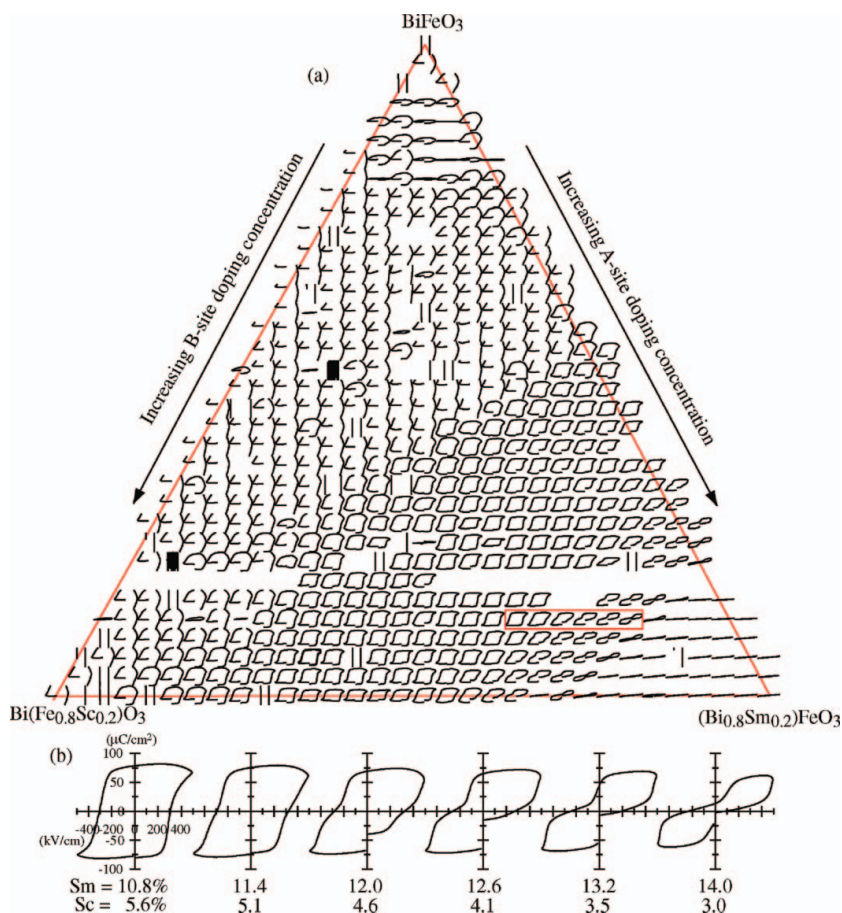
Figure 3. (a) Plot of all polarization hysteresis loops taken from the fabricated library. The loops are arranged according to the position of the top electrode. The all loops are obtained at 5 kHz at room temperature. (b) "Zoom-up" of the hysteresis loops in the red box in (a). (See Color Plate XXXIII)

as 1/2) XRD spots, and remanent polarization P$_r$ in the PE loop as functions of Sm and Sc dopant concentrations in Figs. 4 (a), (b) and (c), respectively. Note that in these plots, the data points which were triangularly distributed on the original library layout have been displaced to more clearly delineate the dependence on the Sm concentration (vertical scale) and the Sc concentration (horizontal scale). It is clear that these three parameters are well described by only the Sm composition and are not dependent on the Sc composition. The 1/4 spot intensity variation is observed to take place as a function of Sm composition (8 to 14%). Beyond Sm 14%, the 1/4 spot disappears, while the
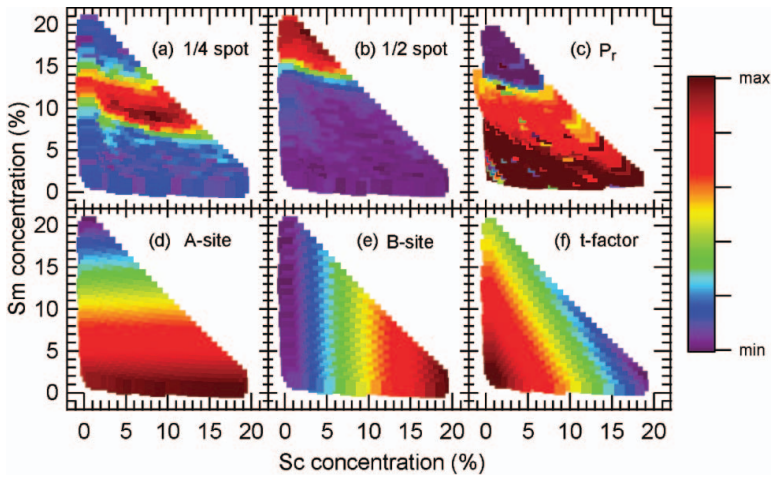
Figure 4. Plots of (a) (0, 1/4, 7/4) (1/4{011}) spot intensity, (b) (0, 1/2, 2) (1/2{010}) spot intensity, (c) remnant polarization P_r, (d) average A-site ionic radius, (e) average B-site ionic radius, and (f) tolerance factor as function of Sm and Sc substitution concentration. In (a), (b) and (c), the maximum (red-hue) and minimum (purple-hue) of the color bar is 1.0 and 0.0 respectively. In (d), the maximum is 1.36 Å and the minimum is 1.344 Å. In (e), the maximum is 0.664 Å and the minimum is 0.645 Å. In (f), the maximum is 0.953 and the minimum is 0.945. (See Color Plate XXXIV)

1/2 spot intensity begins to appear and gets enhanced. This corresponds to the rhombohedral to orthorhombic structural transition. As a consequence of the structural transition, P_r also becomes zero at Sm $\approx$ 14%, indicating that a ferroelectric hysteresis loop has undergone the transition to the double hysteresis loop as seen in Fig. 3(b).

It is interesting to compare the observed trend in the structural and the ferroelectric properties with the changes in average ionic radius in A-site and B-site, and the tolerance factor of which are plotted in Figures 4(d), (e) and (f), respectively. To calculate these parameters in Figs 4(d)-(f), we used 1.36 Å as an ionic radius for the Bi^{3+} ion in 12 coordination, and 1.28 Å for the Sm^{3+} ion [16]. For the Fe^{3+} and Sc^{3+} ions with 6 coordination, 0.745 Å and 0.645 Å are used, respectively. The observed tend in XRD spot intensities and P_r (Figs 4(a)-(c)) essentially agrees with changes in the average A-site ionic radius in Fig 4(d). This indicates that the average A-site radius is the key parameter and that the chemical pressure provided by A-site substitution governs the structural and the ferroelectric properties. It is known that the tolerance-factor is a useful parameter to describe properties in perovskite-structured materials. However in the present case, this does not appear to be the case.

CONCLUSIONS

In summary, we have investigated the structural and ferroelectric properties of the A- and B-site co-doped $BiFeO_3$ thin films by the combinatorial composition spread technique. Scanning 2-dimensional x-ray diffraction reveals that the structural transition from the rhombohedral to the orthorhombic structural phase takes place at 14% Sm dopant in A-site and is not dependent on the Sc concentration in the B-site. The ferroelectric properties also show the concomitant changes with the structural transition, at which the double-hysteresis loop behaviors are observed. Strong dependence of the observed properties on the average A-site ionic radius demonstrates the significance of A-site substitution on $BiFeO_3$.

ACKNOWLEDGMENTS

REFERENCES

1. J. Wang, J. B. Neaton, H. Zheng, V. Nagarajan, S. B. Ogale, B. Liu, D. Viehland, V. Vaithyanathan, D. G. Schlom, U. V. Waghmare, N. A. Spaldin, K. M. Rabe, M. Wuttig, and R. Ramesh, *Science* **299**, 1719 (2003).

2. T. Zhao, A. Scholl F. Zavaliche, K. Lee, M. Barry, A. Doran, M. P. Cruz, Y. H. Chu, C. Ederer, N. A. Spaldin, R. R. Das, D. M. Kim, S. H. Baek, C. B. Eom and R. Ramesh, *Nature Materials* **5**, 823 (2006).

3. Z. Cheng, X. Wang, S. Dou, H. Kimura, and K. Ozawa, *Phys. Rev.* **B 77**, 092101 (2008).

4. G. D. Hua, X. Cheng, W. B. Wu, and C. H. Yang, *Appl. Phys. Lett.* **91**, 232909 (2007).

5. G. L. Yuan, S. W. Or, J. M. Liu, and Z. G. Liu, *Appl. Phys. Lett.* **89**, 052905 (2006).

6. Y. H. Chu, Q. Zhan, C. H. Yang, T. Zhao, M. P. Cruz, L. W. Martin, P. Yu, R. Ramesh, P. T. Joseph, I. N. Lin, W. Tian, and D. G. Schlom, *Appl. Phys. Lett.* **92**, 102909 (2008).

7. A. V. Khomchenko, *Appl. Phys. Lett.* **93**, 262905 (2008).

8. W. M. Zhu, L. W. Su, L. G. Ye, and W. Ren, *Appl. Phys. Lett.* **94**, 142908 (2008).

9. D. Kan, L. Pálová, V. Anbusathaiah, C.-J. Cheng, S. Fujino, V. Nagarajan, K. M. Rabe, and I. Takeuchi, *Adv. Fun. Mater.* in press (2010).

10. S. Fujino, M. Murakami, V. Anbusathaiah, S.-H. Lim, V. Nagarajan, C. J. Fennie, M. Wuttig, L. Salamanca-Riba, and I. Takeuchi, *Appl. Phys. Lett*. **92**, 202904 (2008).

11. V. Nagarajan, A. Stanishevsky, L. Chen, T. Zhao, B.-T. Liu, J. Melngailis, A. L. Roytburd, and R. Ramesh, *Appl. Phys. Lett*. **81**, 4215 (2002).

12. C.-J. Cheng, D. Kan, S.-H. Lim, W. R. McKenzie, P. R. Munroe, L. G. Salamanca-Riba, R. L. Withers, I. Takeuchi, and V. Nagarajan, *Phys. Rev*. **B 80**, 014109 (2009).

13. P. Baettig, C. F. Schelle, R. LeSar, U. V. Waghmare, and N. A. Spaldin, *Chem. Mater*. **17**, 1376 (2005).

14. S. Yasui, H. Uchida, H. Nakaki, K. Nishida, H. Funakubo, and S. Koda, *Appl. Phys. Lett*. **91**, 22906 (2007).

15. A. A. Belik, S. Iikubo, K. Kodama, N. Igawa, S. Shamoto, M. Maie, T. Nagai, Y. Matsui, S. Y. Stefanovich, B. I. Lazoryak, and E. Takayama-Muromachi, J. *Amer. Chem. Soc*. **128**, 706 (2006).

16. Y. Q. Jia, *J. Solid State Chem*. **95**, 184 (1991).